

Failure analysis of gas turbine first stage blade made of nickel-based superalloy

A.M. Kolagar, N. Tabrizi*, M. Cheraghzadeh, M.S. Shahriari

Research & Development, Department of MavadKaran Engineering Company, Mapna Group, Tehran, Iran



ARTICLE INFO

Keywords:

Failure analysis
Gas turbine blade
IN738LC superalloy
Overheating

ABSTRACT

Various degradation mechanisms are characterized in gas turbine rotor blades due to service conditions such as: high temperature and stress. Failure of turbine blade can have the tremendous effects on the safety and performance of the gas turbine engine. This paper investigates a first stage turbine blade failure in a 6.5 MW gas turbine. The blade is made of nickel-based superalloy, and the failure occurred in the airfoils after 6500 h of operation. Several examinations were carried out in order to identify potential failure reasons such as: visual examination, fractography and microstructural characterization used by optical and scanning electron microscopes (SEM) and energy dispersive X-ray (EDX). The precipitated phases morphology (carbides and γ' (Ni₃Al)) changed in the airfoil for example γ' resolved and re-deposited in addition to decomposition of carbides. Furthermore, the fracture surface exhibits the local melting occurred and re-solidified in the leading edge. From analysis and experimental results of this study, overheating is shown to be the main reason of blade failure.

1. Introduction

Rotor blades are critical components of gas turbines in power plants. Operating conditions are such that the high temperature of the gas stream passes over blades and the complex stress is exposed to blades resulting in various degradation mechanisms. When degradation mechanisms become active in blades with time, they can reduce service life. Studies show that the most important failure mechanisms in industrial turbine blades are creep damage, fatigue, corrosion, erosion and environmental attack (oxidation, hot corrosion, erosion and foreign object damage) [1,2]. Some of these modes interrelated and can simultaneously occur. For example, cracking can occur by creep and/or fatigue mechanisms [3,4]. It is well known that creep damage can significantly reduce the fatigue strength and leads to failure of components [4].

In the event of the blade failure, the power plant shuts down, potentially leads in to prolonged outages and economic loss. When this occurs, it is necessary to conduct a detailed failure analysis on turbine blades in order to understand the problem and improve turbine system reliability [5,6].

Over the last few decades, operating temperatures of gas turbine engines have been increased to achieve increased engine power and efficiency. For this reason gas turbine blades are made of nickel-based and cobalt-based superalloys since these materials are able to withstand the combination of high stress and high temperature [7]. Nickel-base superalloys are an unusual class of metallic materials with an exceptional combination of mechanical properties such as high temperature strength, toughness (650–1100 °C), resistance to degradation in corrosive or oxidizing environments [8].

Superalloy IN738LC is one of the most widely used nickel base superalloys utilized to manufacture rotor blades for first stage gas

* Corresponding author.

E-mail address: Tabrizi.Narges@mapnamk.com (N. Tabrizi).

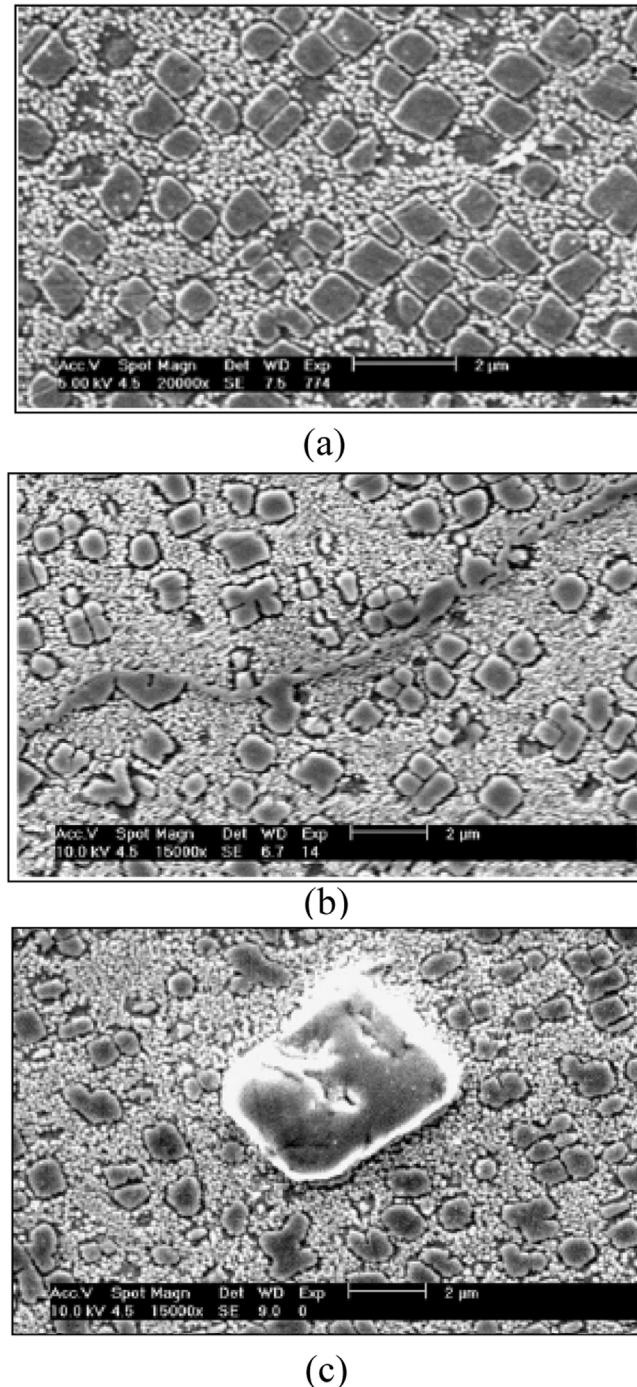


Fig. 1. The microstructure of superalloys IN738LC under standard heat treatment (a) including cubic and spherical γ' precipitates (b) discontinuous carbides in grain boundaries (c) carbide inside grains of γ matrix of new blade [13].

turbines. It is well known that IN738LC has a multiphase microstructure and owns its high temperature strength from the precipitate of γ' intermetallic compound phase (Ni_3Al), FCC nickel base solid solution matrix, carbide phases such MC inside grain and M_{23}C_6 formed through grain boundary. MC carbide may include some elements such as Ti, refractory elements like W, Ta and a little Cr, Ni [8,9]. Significant amount of bulk-like MC type carbides are mainly precipitated during solidification of alloys, while the precipitate M_{23}C_6 in alloys are mainly deposited from the matrix along the boundaries during heat treatment and service (at 760–980 °C) [10]. This type of carbide is formed due to super-saturation of carbon in the matrix and degeneration of the MC type carbide. The equation of decomposition is as follows:

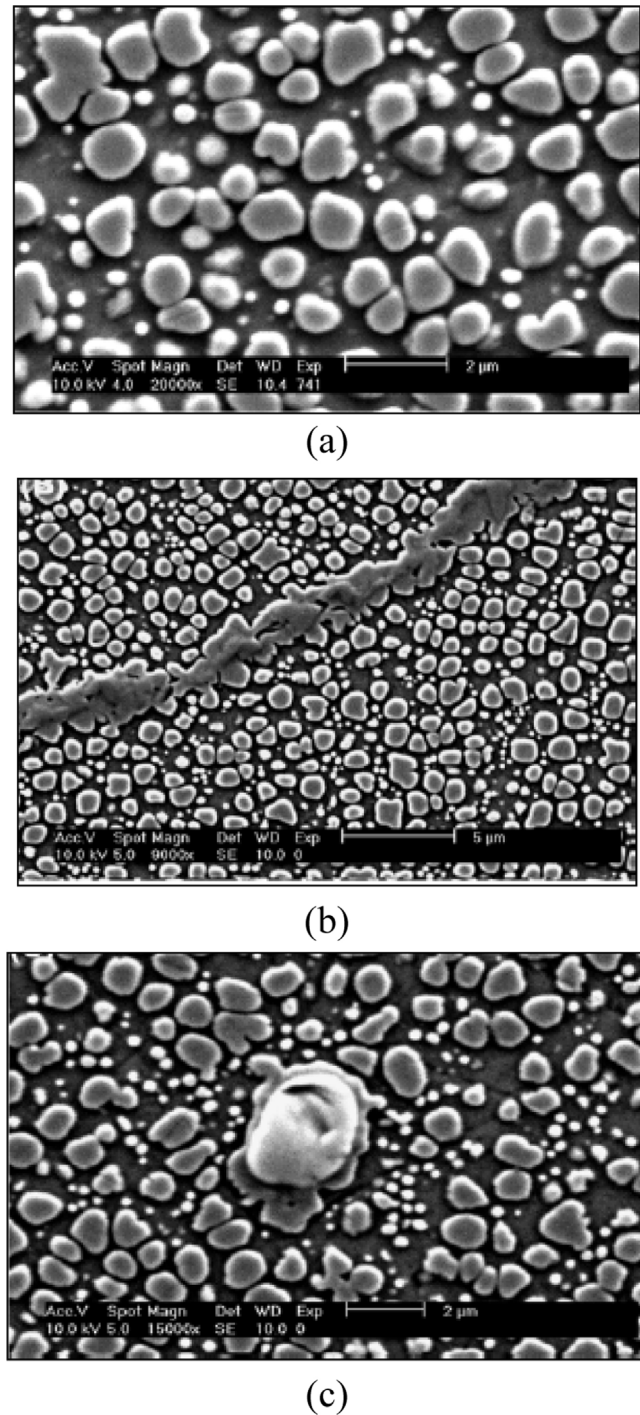


Fig. 2. The microstructure of superalloys IN738LC exposed under the damage due to long time service (a): coarsening γ' (formed irregular γ'), (b): formed continuous carbide in grain boundary, (c): decomposition of MC carbide in used blade [13].



In this carbide (M_{23}C_6), M can be Cr, W and Mo. The morphology of this carbide is observed as discontinuous films in grain boundaries. Fig. 1 shows the microstructure of IN738LC under heat treatment including γ' precipitates (Fig. 1(a)), M_{23}C_6 carbides along grain boundary (Fig. 1(b)) and MC grain interior. Due to pinning effect of the sphere-like M_{23}C_6 carbides precipitated along boundaries may restrain the sliding of boundaries hence, creep resistance of alloys may be improved. Moreover, the granular M_{23}C_6 carbides distributed along boundaries may delay the propagation rate of cracks. During operation of Ni based superalloys at high



Fig. 3. Damaged rotor blades of first-stage turbine blades after 6500 h of operation at about 750–800 °C a 6.5 MW gas turbine.

temperature, the size, distribution and the space between γ' and carbides in grain boundaries and grain interior changes. [Fig. 2](#) shows the change of microstructure of IN738LC exposed under damage due to long service time: [Fig. 2\(a\)](#): coarsening γ' (formed irregular γ'), [Fig. 2\(b\)](#): continuous carbide formed in grain boundary, [Fig. 2\(c\)](#): decomposition of MC carbide [11,12,13].

As the microstructure affects the tensile and creep properties, the change of morphology of precipitated phases especially γ' is one of the damage mechanisms that leads to the microstructure degradation and the reduction of the mechanical properties [14]. Hereby, in this paper, characterization methods (optical and scanning electron microscopes (SEM) and energy dispersive X-ray (EDX)) were used to analyse failure reasons of first-stage turbine blades based on IN738LC studied after 6500 h of operation in a 6.5 MW gas turbine.

2. Experimental work

In this paper, the damaged first-stage turbine blades (IN738LC) were used to investigate after 6500 h of operation at about 750–800 °C in a 6.5 MW gas turbine. [Fig. 3](#) shows the damaged turbine blades. The blades are designed without cooling channels and coating. The visual inspections of blades indicate that the damage pattern for each blade was observed to be reasonably consistent in all blades, the blade tip portions having fractured from the main airfoil body ([Fig. 3](#)). The surface colour change in this area proves that the oxidation occurred.

The chemical composition of the alloy used is given in [Table 1](#). To investigate the microstructure, the test pieces were prepared from the airfoil and root of the blade, as in [Fig. 4](#). They were ground by 600, 800, 1200 grit papers and subsequently fine polished with diamond pastes 3 and 1 microns. Then the samples were etched by using oxalic solution including oxalic acid (10 mg) and distilled water (100 ml). Morphology, size of γ' and change of the microstructure under service condition were studied by optical microscopy (Lecia DM2500M) and scanning electron microscopy (Zeiss EVO MA 10). The results then analysed with image processing software. In order to investigate the fracture surface, SEM was applied and an EDX probe was used to analyse the local chemistry of carbides.

3. Results and discussion

3.1. Microstructural characterization

Optical images were used to examine the distribution of carbides. [Fig. 5\(a–d\)](#) show the microstructure of the damaged first-stage

Table 1
Chemical composition of IN738LC (wt%).

Ni	B	Zr	Ti	Al	W	Ta	Fe	Co	Mo	Cr	C
Bal.	0.01	0.05	3.5	3.5	2.5	1.7	0.3	8.5	1.7	15.5	0.09

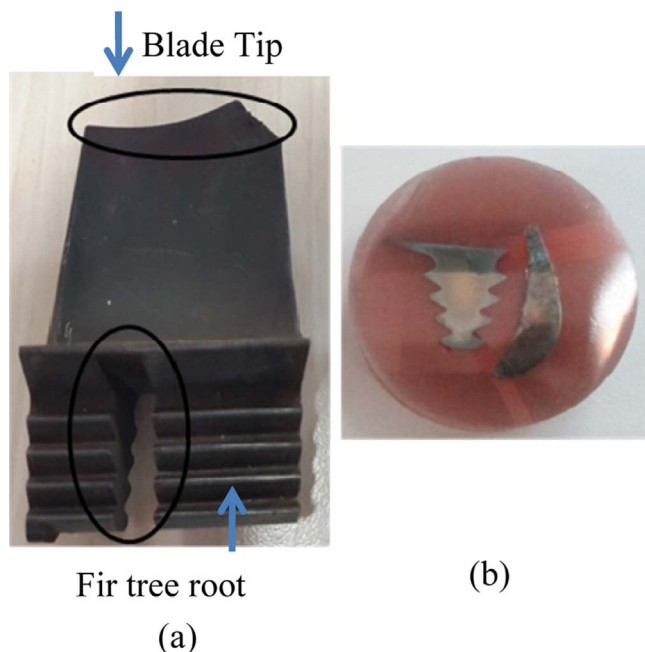
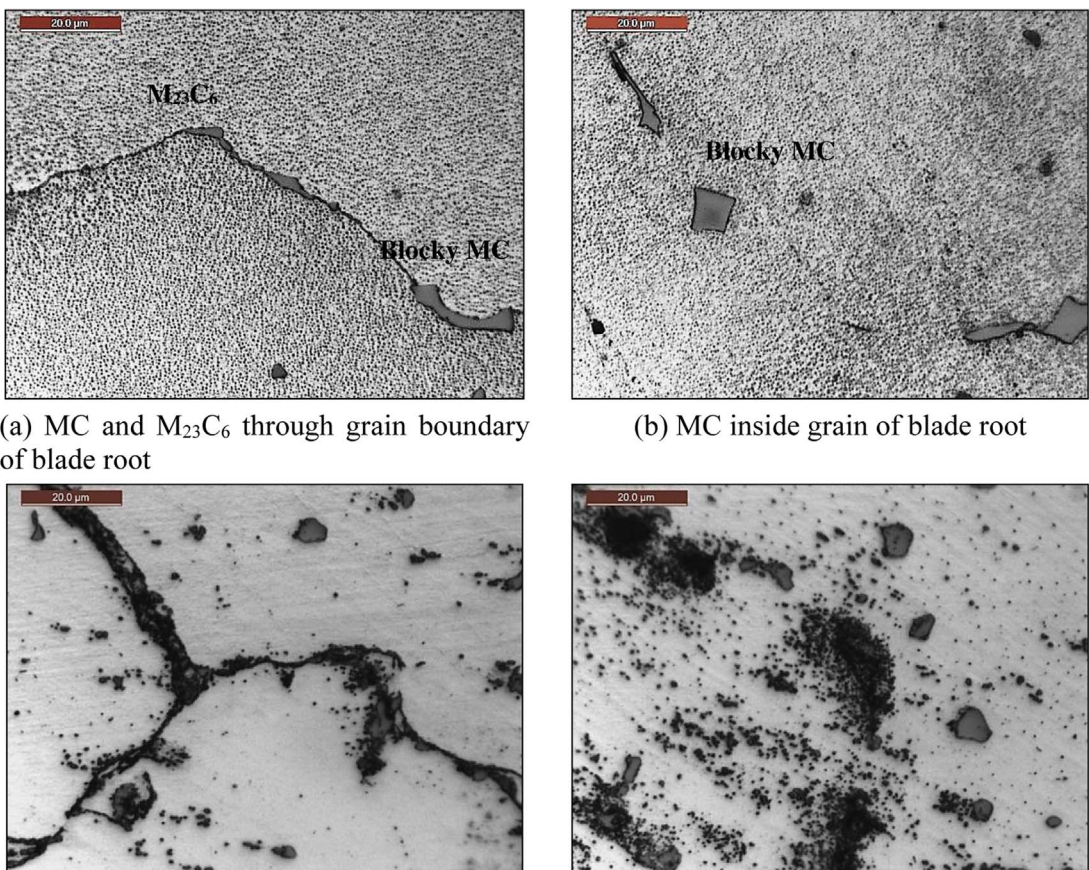
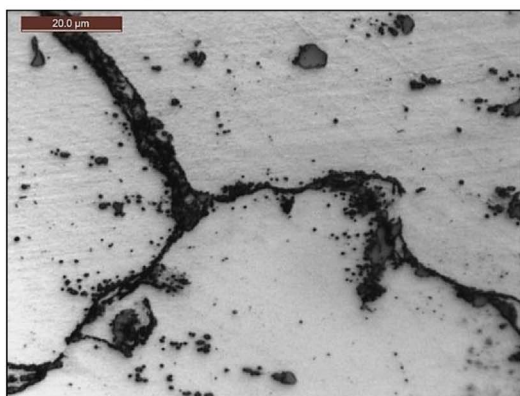


Fig. 4. Prepared Metallography samples of rotor blades of first-stage turbine blades after 6500 h of operation (a) location of prepared samples (b) mounted samples.

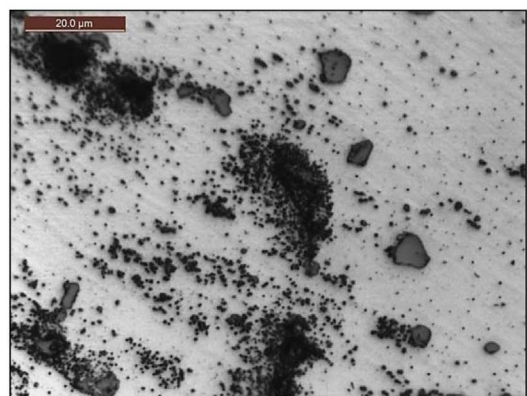


(a) MC and $M_{23}C_6$ through grain boundary of blade root

(b) MC inside grain of blade root



(c) $M_{23}C_6$ through grain boundary of blade airfoil



(d) fine MC in grain of blade airfoil

Fig. 5. The optical image of microstructure of blade (a and b) root and (c and d) airfoil including MC in grain and $M_{23}C_6$ through grain boundary.

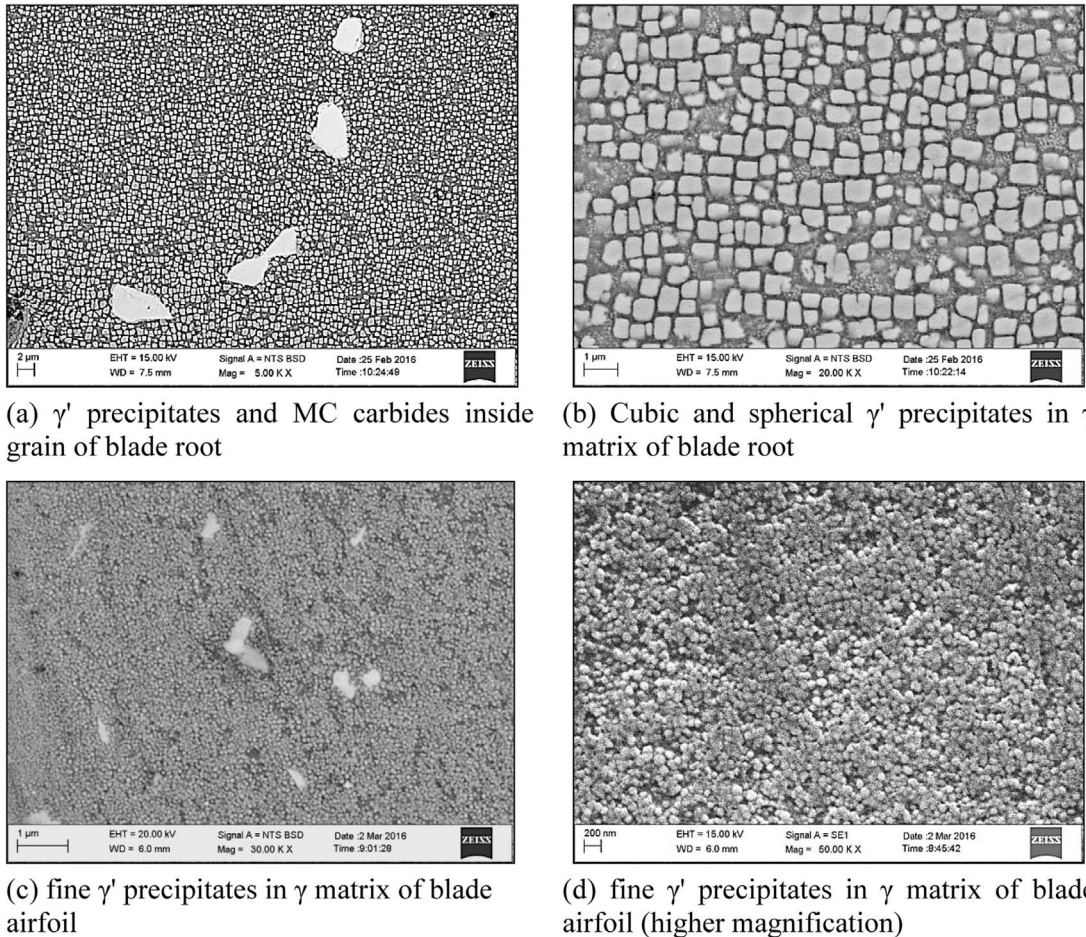


Fig. 6. SEM images of microstructure of blade (a and b) root including cubic, spherical γ' precipitates and MC carbides in grain of γ matrix and MC carbides inside grain of blade root (c and d) airfoil including very fine spherical γ' precipitates in γ matrix.

turbine blade root (a and b) and airfoil (c and d). Various precipitated phases are observed such as carbides: MC carbides inside of the grains and grain boundary; discontinuous M₂₃C₆ in grain boundaries

Different distributions of carbides are detected in the airfoil of blades, Fig. 5(c and d) are compared to Fig. 5(a and b) blade root. Most M₂₃C₆ carbides are seen as discontinuous in grain boundary of root while in airfoil microstructure, the flaky shape of M₂₃C₆ is seen in grain boundary and inside the grains. According to Eq. (1), M₂₃C₆ may result of the MC type carbide decomposition under service. However, some MC carbides remained after service. In Fig. 5(a and b), γ' is observed, small grey points in root but in Fig. 5(c and d) taken in the same scale, no γ' is detected in the airfoil indicating the size of the γ' should be smaller than that of in root. This condition is a result of proposed γ' solution and reprecipitation in airfoil area.

SEM images are shown in Fig. 6(a-d). Comparison between blade root (Fig. 6(a and b)) and airfoil (Fig. 6(c and d)) microstructures confirm the optical microscopy observations that is there is a significant difference between γ' size; very fine γ' in

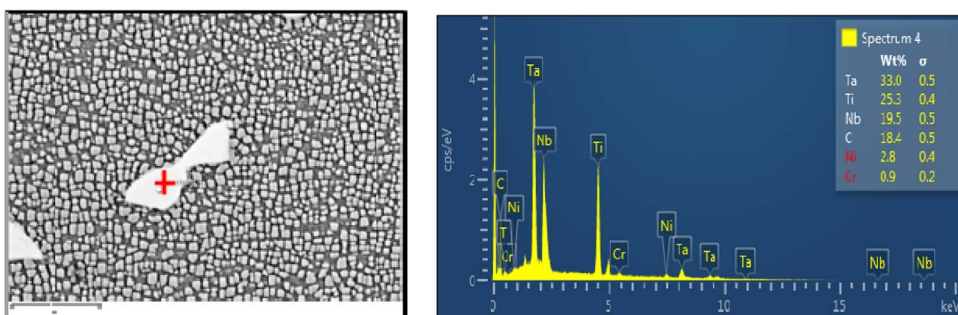


Fig. 7. EDX results of MC in blade after 6500 h of operation.

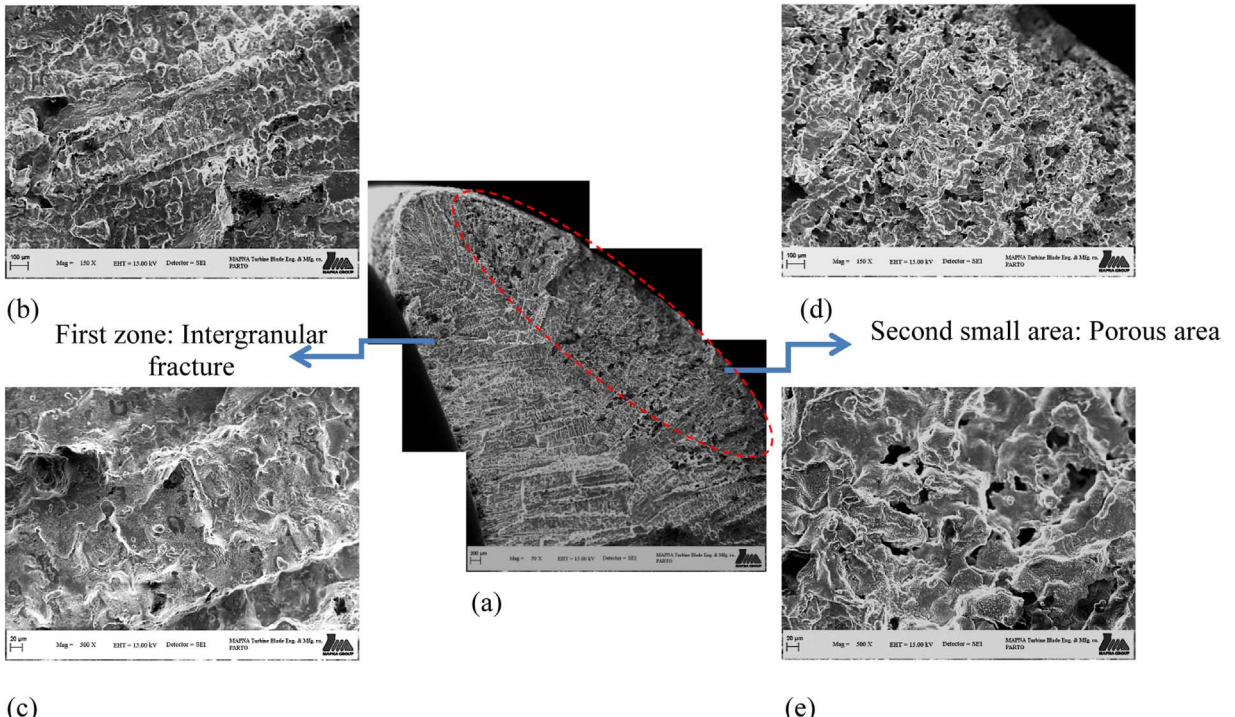


Fig. 8. Secondary electron images illustrating the fracture surface of the blade tip, mostly occurred by Intergranular fracture (a) fracture surface of blade tip; (b and c) dendritic area (Intergranular failure mode); (d and e) porous area (local melting).

blade airfoil. As the blade has just worked 6500 h of operation (expected failure time: 20,000 h), this microstructure is unexpected. The service condition of airfoil (750–800 °C/80 MPa) leads to the occurred creep in this region while stress and temperature are respectively higher and lower in blade root. In airfoil, the primary γ' should be coarsened, moreover the gradual decomposition of MC carbides in matrix and the continuous carbides in grain boundaries should be appeared. But these changes are not observed in airfoil, Fig. 6(c and d). γ' size is measured to be about 50 nm which is extremely smaller than size of γ' in blade root, 500 nm.

The chemical composition of carbides (marked by +) is characterized with EDX. Fig. 7 shows the elements: Ti, Ta and Nb in carbide. Therefore, the type of carbide is determined as MC [8,9].

3.2. Fractography

The fracture surfaces were examined using a SEM. The examination of the blade tip fracture surfaces from the blade revealed no

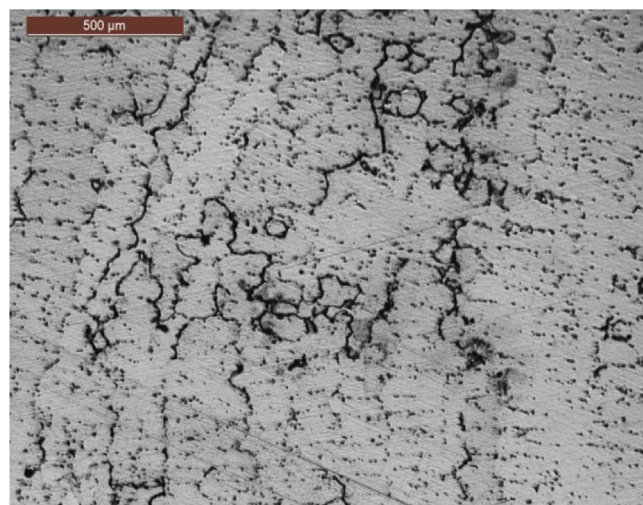


Fig. 9. Optical image of area close to fracture area including discontinuous cracks in grain boundary.

obvious evidence of fatigue (fatigue striation) or any other such form of progressive failure mechanism (Fig. 8(a–e)). The fracture surface shows two zones: the first zone shows intergranular fracture (interdendritic area), typically final stage failure, the dendrites which grew from edges of blade into center. The second small area shows local melting occurred and re-solidified as sponge texture. The small porous area seen in the leading edge is evidence of overheating of gas turbine (marked by red dashed line).

This conjecture is supported by observations made using optical microscope of area located close to the failure region. Fig. 9 shows many cracks nucleated in the interdendritic area and grew along the grain boundaries (intergranular fracture).

The analysis of the blade airfoil, root microstructure and fractography results shows that the hot section temperature of gas turbine increased for unknown amount of time (overheating). The blades were confronted to higher temperature compared to service temperature (750 °C). The size and distribution of γ' in the airfoil (Fig. 6(c and d)) show that these precipitates dissolved in the matrix and re-deposited during shut down of the turbine. Therefore, the temperature should be around solution temperature of γ' , nearby 1160 °C. Furthermore, the optical images of airfoil (Fig. 5(d)) shows the decomposition of MC to $M_{23}C_6$ and remained some MC. Also the temperature should be less than the melting temperature of MC (1250 °C the temperature of partial solution or the initial melting temperature). Moreover, the local melting area in airfoil, confirms this assumption. The temperature of overheating should be above 1000 °C.

4. Conclusions

The following conclusions can be drawn from this study:

1. The microstructure of the damaged rotor fist-stage blade root includes primary and secondary γ' , MC in grain and $M_{23}C_6$ distributed discontinuously through grain boundary, similar to that of new blade and previous studies. Also, the damaged rotor blade has the acceptable initial microstructure.
2. In normal service conditions, it is expected that the primary γ' should be coarsened, moreover the gradual decomposition of MC carbides into $M_{23}C_6$ in matrix and the formation of the continuous carbides in grain boundaries appeared. But SEM images did not confirm the expectations and emphasizes the abnormal conditions. Increasing the service temperature leads to precipitates dissolved in the matrix and re-deposited during shut down of the turbine. Furthermore, the fractography observation confirms local melting in the leading edge.
3. Changes of the first-stage airfoil blade microstructure and local melting of blade indicates that the blades were overheated for unknown period of time. The blades were exposed to higher temperature of above 1000 °C.

Acknowledgments

The authors would like to acknowledge the colleagues in MavadKaran Company for their great cooperation and extensive help. Moreover, the authors would like to show their appreciation for MAPNA Group's support in this research.

References

- [1] Schilke PW. GE power system. Gen Electr Co Rep 1980;1–18. M-715.
- [2] Strang. GE power system. Gen Electr Co Rep 2000;319–32. M-912.
- [3] Carter TJ. Common failures in gas turbine blades. Eng Fail Anal 2005;12:237–47.
- [4] Koul AK, Imariageon JP, Parameswaran VR, Wallace W. Advances in high temperature structural materials and coatings. Ottawa: A publication from national research council of Canada; 1994.
- [5] Wang W, Xuan F. Failure analysis of the final stage blade in steam turbine. J Eng Fail Anal 2007;14:632–41.
- [6] Vardar N, Ekerim A. Failure analysis of gas turbine blades in a thermal power plant. J Eng Fail Anal 2007;14:743–9.
- [7] Bhawmik SK, Sujata M. Failure of a low pressure turbine rotor blade of an aero engine. J Eng Fail Anal 2006;13:1202–19.
- [8] Steven RA, Flewthorpe PEJ. Intermediate regenerative heat treatment for extending the creep life of superalloy IN738. Mater Sci Eng 1981;50:271–84.
- [9] Davin A, Mertens CL, Vierset P, Louis P. Microstructural damage induced during the repair. Process proceeding of a conference. 1986; 1986. p. 811–20. D. Reidel Publishing Co.
- [10] Chang E, Chou JC. Microporosity in an investment-casting turbine blade of IN713LC superalloy. AFS Trans 1987;95:749–54.
- [11] Decker RF, Sims CT, Hagel WC. The superalloy I. New York: John Wiley & Sons; 1984. p. 33–7.
- [12] Ross EW, Sims CT. Nickel base superalloys superalloy II. New York: John Wiley & Sons; 1987. p. 97–113.
- [13] Hosseini S, et al. Microstructural evolution in damaged IN738LC alloy during various of rejuvenation heat treatments steps. J Alloys Compd 2012;512:340–50.
- [14] Koul AK, Imariageon JP, Castillo R. 1988 rejuvenation of service-exposed IN738 turbine blades. Superalloy 1988;75:5–764.